

Short communication

Controlled microwave-assisted synthesis of ZnO nanopowder and its catalytic activity for *O*-acylation of alcohol and phenol

Firouz Matloubi Moghaddam*, Hamdollah Saeidian

Department of Chemistry, Sharif University of Technology, P.O. Box 11365-9516, Tehran, Iran

Received 2 December 2006; received in revised form 19 February 2007; accepted 4 March 2007

Abstract

ZnO nanopowder has been successfully synthesized by a microwave-assisted solution approach using $\text{Zn}(\text{CH}_3\text{CO}_2)_2 \cdot 2\text{H}_2\text{O}$ and NaOH. The results obtained from X-ray diffraction (XRD), scanning electron microscopy (SEM) and transition electron microscope (TEM) show that the mean particle size is 30 nm. SEM and TEM micrographs of ZnO nanopowder also reveal that nanoparticles have spherical shape. Catalytic activity of ZnO nanopowder for *O*-acylation of alcohol and phenol has been investigated. The results show that the reaction time by using ZnO nanopowder has been reduced by almost 24 times with higher yield than ZnO bulk.

© 2007 Published by Elsevier B.V.

Keywords: Zinc oxide; Nanopowder; Controlled microwave heating; Catalyst activity; Acylation

1. Introduction

Development of new routes for the synthesis of solids is an integral aspect of materials chemistry and physics. Some of the important reasons for this are the continuing need for fast and energy-efficient techniques, and necessity to avoid competing reactions in the known processes. Recently, a new deposition technique has reported: microwave activated chemical bath deposition (MW-CBD). This technique is based on the microwave heating of a precursor solution in which the substrate is immersed [1–4]. Microwave-solvothermal synthesis is generally quite faster, simpler and more energy efficient. The exact nature of microwave interaction with reactants during the synthesis of materials is somewhat unclear and speculative. Energy transfer from microwave to the material is believed to occur either through resonance or relaxation, which results in rapid heating. This knowledge is widely used as the basis in the discussion of the reaction mechanism.

On the other hand, ZnO is an interesting multifunctional material for its promising applications in solar energy transformation, sensors, optoelectronic devices and photocatalysis [5–8]. Although different methods such as Sol–Gel, atomic layer deposition, laser heating, polymer stabilization [9–12]

have already been developed for the fabrication of ZnO with various morphologies and size, only a few studies have been reported on the preparation of nanocrystalline and bulk ZnO powder by microwave heating [13–16].

Solution-phase methods have become widely used for the synthesis of crystalline nanoparticles [17–19]. In most cases, these techniques involve nucleation and growth from homogeneous solution. Processes, such as coarsening and aggregation can compete with nucleation and growth in modifying the particle size distribution in these methods. In this work, three strategies have been used to arrest growth:

- It has been reported that the solvent used for the synthesis is strongly adsorbed onto the nanoparticles, so that growth suppressed soon after nucleation. For example, alcohols are suitable solvents for synthesis of ZnO nanoparticles [20]. On the other hand, in aqueous solution, growth usually proceeds rapidly with the formation of relatively large particles. Therefore, we used 2-propanol as a nonaqueous solvent for the synthesis of ZnO nanoparticles.
- Since the micelles [21], capping agents [22] and polymer stabilization [12] could be used to arrest the growth, we used zinc acetate as the precursor, since acetate ion can act as the capping agent [17].
- In most cases, nucleation and growth of nanoparticles are allowed to take place over an extended period of time at

* Corresponding author.

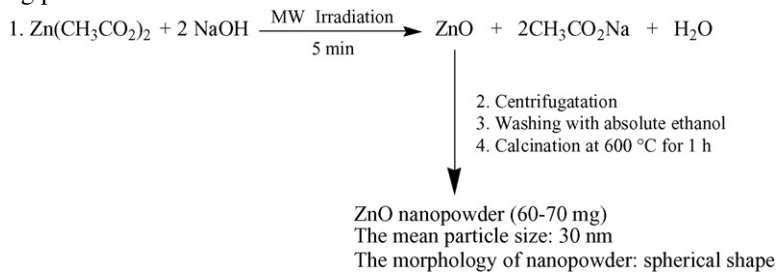
E-mail address: matloubi@sharif.edu (F.M. Moghaddam).

a moderate temperature, yielding a wide range of sizes. Thus, homogeneous heating of precursor during a short time by controlled microwave heating has been used to achieve a narrow distribution of sizes. To explore potential ability of microwave as an energy source for synthesis [23–27], in this paper, the application of controlled microwave heating for the synthesis of ZnO nanopowder using $\text{Zn}(\text{CH}_3\text{CO}_2)_2 \cdot 2\text{H}_2\text{O}$ in 2-propanol has been discussed. The catalytic activity of ZnO nanopowder for *O*-acylation of alcohol and phenol has also been studied.

2. Experimental

2.1. Sample preparation

The ZnO nanopowder was prepared according to the following processes:



In a typical procedure, 0.22 g (1 mmol) of $\text{Zn}(\text{CH}_3\text{CO}_2)_2 \cdot 2\text{H}_2\text{O}$ was suspended in 120 mL of 2-propanol under vigorous stirring at 50 °C. A sodium hydroxide alcoholic solution was prepared by adding 0.08 g (2 mmol) NaOH to 30 mL of 2-propanol under vigorous stirring at 50 °C. The flasks containing $\text{Zn}(\text{CH}_3\text{CO}_2)_2 \cdot 2\text{H}_2\text{O}$ and NaOH alcoholic solution were cooled in an ice-water bath. The sodium hydroxide solution was then added to zinc acetate solution under vigorous stirring to give a total volume of 150 mL. Final solution was heated in a controlled microwave cavity for 5 min. During the microwave irradiation the temperature of the solution reached up 80 °C. After 5 min, the transparent solution obtained. The centrifugation of transparent solution yields white products, which washed twice with absolute ethanol and dried at 70 °C for 4 h. Then white powders calcined at 600 °C for 1 h. The yield of ZnO nanopowder after washing and drying is about 70% (60–70 mg).

2.2. Apparatus and characterization

The microwave-assisted reactions were performed in a single-mode microwave cavity (Ethos, MR, 2.45 GHz, maximum power 1000 W), producing controlled irradiation. Reaction temperatures were determined and controlled via the built-in, on-line sensor. The microwave synthesis reactor was equipped with a water-cooled condenser.

Absorption spectra were obtained using a Shimadzu UV-vis spectrophotometer. X-ray diffraction (XRD) was performed with a Siemens D5000 X-ray diffractometer using graphite-monochromatized high-intensity Cu K α radiation ($\lambda = 1.5406 \text{ \AA}$). Scanning electron microscopy (SEM) images

were obtained using a Stereo Scan 3360 Leica Cambridge. Fourier transform infrared spectroscopy (FT-IR) was performed using a Nicolet (Magna 500). A JEOL JEM-2010 transition electron microscope (TEM) was used for determining the average particle size and morphology of the powders on an accelerating voltage of 200 kV.

3. Results and discussion

3.1. UV-vis absorption

Before centrifugation and calcinations of the transparent solution, the produced ZnO was checked with UV-vis spectra and has found that the product has nanostructure.

Fig. 1 shows absorption spectra for the growth of ZnO in 2-propanol under controlled microwave heating at 80 °C for 5

and 10 min. In both cases, the absorption onset is significantly blue-shifted compared to the absorption onset for bulk zinc oxide at about 385 nm, showing that the average particles size is in the quantum regime. The average particle size in the transparent solution was obtained from the inflection point of the absorption edge using the effective mass model [20], which was in the range of 7–10 nm.

From the spectra shown in Fig. 1, we can conclude that nucleation and growth are completed after 5 min under controlled microwave heating (Fig. 1a). After 10 min, size distribution of nanoparticles has become broad (Fig. 1b). Solution involving ZnO sols is translucent for 50 days. UV-vis spectra after 50 days show that sols are stable (Fig. 1c); therefore, 2-propanol and acetate ions can act as capping reagent. White precipitates appeared in solution after 50 days.

Since colloidal nanoparticles are dispersed in solution, they are not bound to any solid support. Therefore, they can be produced in large quantities in a reaction flask and then can be transferred to any desired substrate or object. It is, for example, possible to coat their surface with biological molecules such as proteins. In this way it has been possible to label specific compartments of a cell with different types of nanoparticles [28].

3.2. X-ray diffraction

Fig. 2 shows XRD pattern of the calcined ZnO nanopowder which is a typical zincite peak pattern with lattice constants $a = 3.249 \text{ \AA}$ and $c = 5.206 \text{ \AA}$ [29]. According to this pattern no impurities could be find in the powder, indicating that they have been completely removed using the washing procedure. The

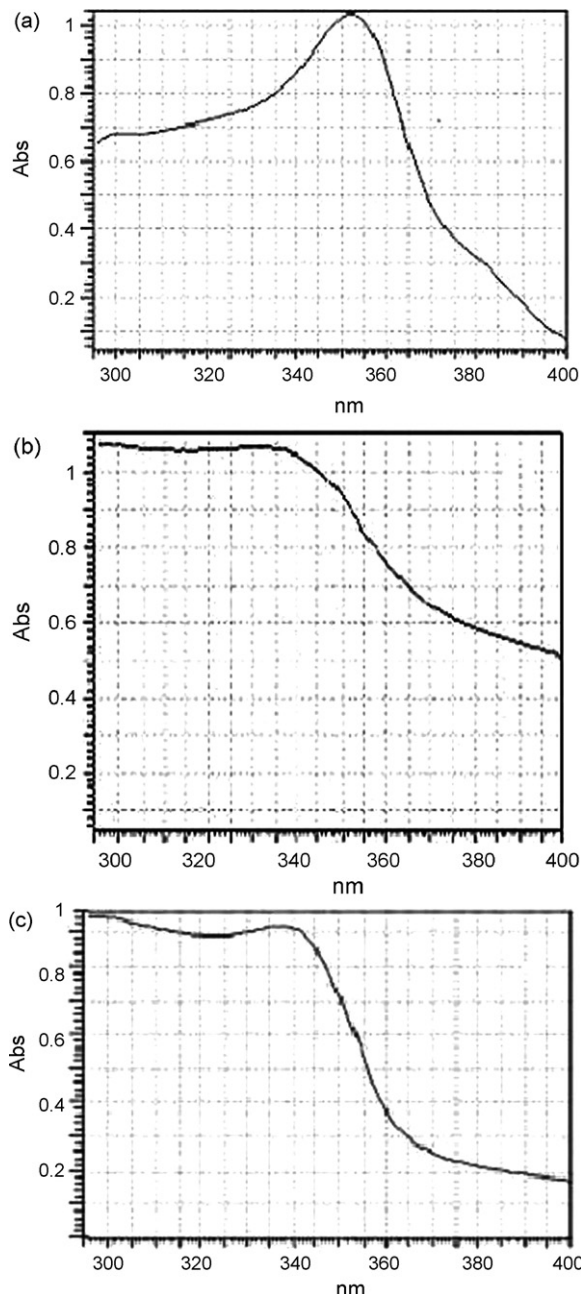


Fig. 1. UV-vis absorbance spectra of ZnO sols under controlled microwave heating: (a) 5 min, (b) 10 min and (c) 50 days.

mean particle size was calculated for the ZnO crystallized using the Scherrer's equation [30], $D = (K\lambda)/\beta(\cos \theta)$, on the reflections with (1 0 0), (0 0 2) and (1 0 1), where K is the shape factor of the average crystallite, λ the wavelength for the $K\alpha_1$ component of the employed copper radiation (1.54056 \AA), β the corrected full width at half maximum (FWHM) and θ is the Bragg's angle. The crystallite size of the powder particles is calculated as about 30 nm. This value agreed well with SEM and TEM observations of the ZnO nanopowder. The smaller particles of the ZnO with high purity and short reaction times are the significant advantages of this procedure as compared with the other reported methods [31–32].

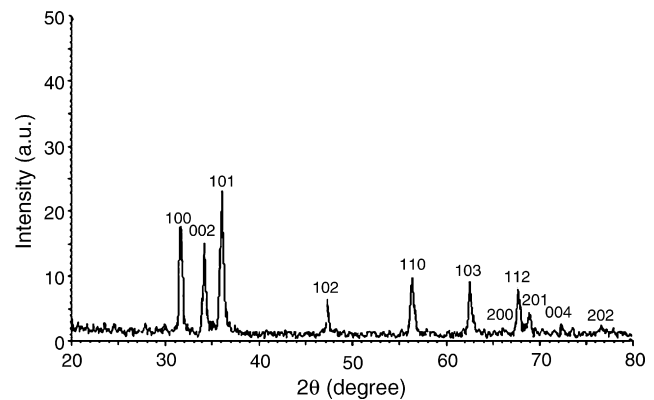


Fig. 2. XRD pattern of the ZnO nanopowder calcined at 600°C for 1 h.

3.3. Fourier transform infrared spectroscopy

The formation of ZnO zincite structure in the synthesized ZnO nanopowder was further supported by FT-IR spectrum as shown in Fig. 3. Almost all functional groups in a molecule characteristically absorb within a definite range of frequency in this technique. Infrared transmission spectrum of ZnO nanopowder was recorded to be in the range of $4000\text{--}400 \text{ cm}^{-1}$. The adsorption band at 492.7 cm^{-1} is the stretching mode of ZnO [33].

3.4. SEM and TEM observations

The morphology of the ZnO nanopowder was investigated by SEM and TEM. As shown in Fig. 4, ZnO particles possess spherical morphology and a narrow distribution of sizes with a 40–50 average diameter, which is higher than those determined by the effective mass model from UV-vis spectra (7–10 nm). The separation of 2-propanol not only resulted in large particle size but also produced subsequent growth and aggregation of several powder particles. However, particles have a narrow nanosized distribution and homogeneous shape after separation of solvent. The regular distribution of nanoparticles is attributed to the uniform temperature gradient maintained on the substrate by controlled microwave heating.

3.5. Evaluation of catalytic activity of ZnO nanopowder for O-acylation alcohol and phenol

Surface of metal oxides exhibit both Lewis acid and Lewis base character [34]. This is characteristic of many metal oxides,

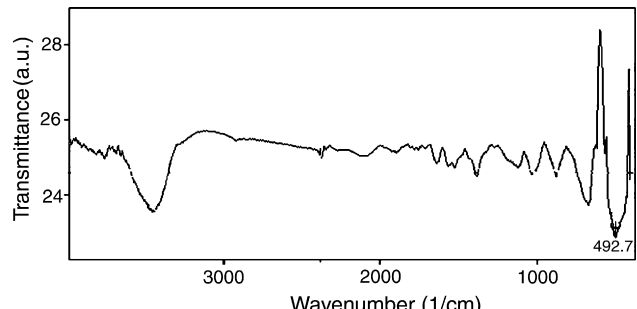


Fig. 3. FT-IR spectrum of ZnO nanopowder.

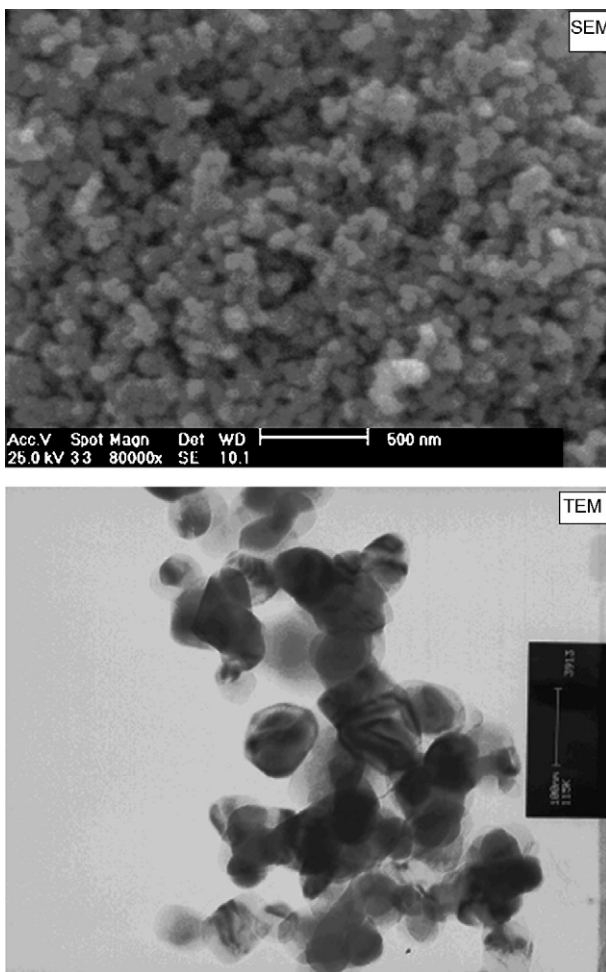
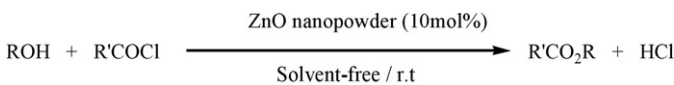


Fig. 4. SEM and TEM micrographs of the ZnO nanopowder calcined at 600 °C for 1 h.

especially TiO_2 , Al_2O_3 , ZnO , etc., and they are excellent adsorbents for a wide variety of organic compounds and increased reactivity of the reactants. Numerous catalytic processes have been discovered that depend on the solid acid and solid base properties of these materials [34]. In any metal oxide, surface atoms make a distinct contribution to its catalyst activity. In powder particles the number of surface atoms is a large fraction of the total. Therefore, catalytic activity of nanopowder was more than that of bulk powders.

ZnO bulk is certainly one of the most interesting of metal oxides, because it has surface properties, which suggest that a very rich organic chemistry may occur there [35–37]. We report herein, our results on *O*-acylation of alcohol and phenol using catalytic amount of ZnO nanopowder at room temperature under solvent-free conditions (Scheme 1). To the best of our



R: phenyl, isopropyl
R': phenyl, methyl

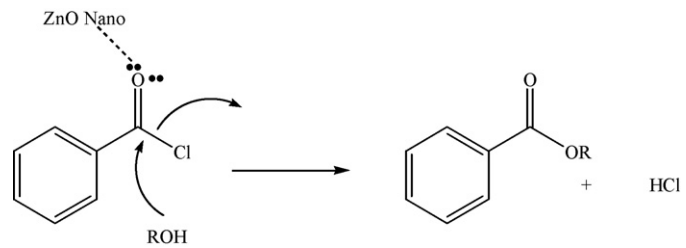
Scheme 1.

Table 1

The results of *O*-acylation of alcohol and phenol using ZnO nanopowder

Entry	R	R'	Catalyst	Reaction time (min)	Yield (%)
1	Phenyl	Phenyl	No catalyst	240	Trace
2	Isopropyl	Phenyl	No catalyst	240	Trace
3	Phenyl	Phenyl	ZnO bulk	120	65
4	Phenyl	Phenyl	ZnO nano	5	92
5	Isopropyl	Phenyl	ZnO bulk	60	83
6	Isopropyl	Phenyl	ZnO nano	5	96
7	Phenyl	Methyl	ZnO bulk	60	90 ^a
8	Phenyl	Methyl	ZnO nano	5	95
9	Isopropyl	Methyl	ZnO bulk	30	95
10	Isopropyl	Methyl	ZnO nano	5	96

^a The result of reference [35].



Scheme 2.

knowledge, this is the first demonstration of the ZnO nanopowder based-acylation.

In the absence of ZnO , no reaction was observed within 240 min, while good results were obtained in the presence of ZnO nanoparticle. Clearly, the reaction time using ZnO nanopowder has been reduced by almost 24 times with higher yield than ZnO bulk (92% versus 65%, Table 1). The products are known and were identified by comparison of their physical and spectral data (^1H NMR, ^{13}C NMR) with those of authentic samples.

At *O*-acylation of the alcohol and/or the phenol, ZnO is coordinated to the oxygen of the acyl chloride, resulting in the increased reactivity of acyl chloride (Scheme 2). ZnO nanopowder is coordinated better than ZnO bulk, while the ZnO nanopowder has more surface atoms, participating at the reaction.

4. Conclusions

ZnO nanopowder was successfully synthesized by an efficient and simple controlled microwave-assisted approach using $\text{Zn}(\text{CH}_3\text{COO})_2 \cdot 2\text{H}_2\text{O}$ and NaOH . Reaction time and separation of solvent have significant influences on the size of ZnO nanopowder. The absorption edge of ZnO sols showed a strong blue shift. The XRD peaks revealed good crystalline of the nanoparticles with the mean particle size 30 nm. SEM and TEM images show spherical morphology for ZnO nanopowder. ZnO nanopowder has strong catalytic activity for *O*-acylation of alcohols and phenols. Current efforts in our research group are attempting to expand the application of the controlled microwave heating for synthesizing other metal oxides

and using nanopowders especially ZnO for catalyzed organic reactions.

References

- [1] K.J. Rao, P.D. Ramesh, *Bull. Mater. Sci.* 18 (1995) 447.
- [2] Y.J. Zhu, W.W. Wang, R.J. Qi, X.L. Hu, *Angew. Chem. Int. Ed.* 43 (2004) 1410.
- [3] W.W. Wang, Y.J. Zhu, G.F. Cheng, Y.H. Huang, *Mater. Lett.* 60 (2006) 609.
- [4] M. Shao, Q. Li, B. Xie, J. Wu, Y. Qian, *Mater. Chem. Phys.* 78 (2002) 288.
- [5] K. Keis, L. Vayssières, S.E. Lindquist, A. Hagfeldt, *Nanostruct. Mater.* 12 (1999) 487.
- [6] E. Comini, G. Faglia, G. Sberveglieri, Z.W. Pan, Z.L. Wang, *Appl. Phys. Lett.* 81 (2003) 1869.
- [7] Y. Chen, D. Bagnal, T. Yao, *Mater. Sci. Eng. B* 75 (2000) 190.
- [8] D. Han, X.L. Ren, D. Chen, F.Q. Tang, D. Wang, J. Ren, *Photogr. Sci. Photochem.* 23 (2005) 414.
- [9] L. Spanhel, M.A. Anderson, *J. Am. Chem. Soc.* 113 (1991) 2833.
- [10] J. Liu, X. Hung, Y. Li, J. Duan, H. Ai, L. Ren, *Mater. Sci. Eng. B* 127 (2006) 85.
- [11] R. Wu, C. Xie, H. Xia, J. Hu, A. Wang, *J. Cryst. Growth* 217 (2000) 274.
- [12] A. Taubert, G. Glasser, D. Palms, *Langmuir* 18 (2002) 4488.
- [13] X.L. Hu, Y.J. Zhu, S.W. Wang, *Mater. Chem. Phys.* 88 (2004) 424.
- [14] S. Komarneni, M. Bruno, E. Mariani, *Mater. Res. Bull.* 35 (2000) 1843.
- [15] W.W. Wang, Y.J. Zho, *Inorg. Chem. Commun.* 7 (2004) 1003.
- [16] K. Sridhar, M. Bruna, E. Mariani, *Mater. Res. Bull.* 35 (2000) 1843.
- [17] Z. Hu, G. Oskam, R.L. Penn, N. Pesika, P.C. Searson, *J. Phys. Chem. B* 107 (2003) 3124.
- [18] C.B. Murray, C.R. Kagan, M.G. Bawendi, *Annu. Rev. Mater. Sci.* 30 (2000) 545.
- [19] A.V. Murugan, R.S. Sonawane, B.B. Kale, S.K. Apte, A.V. Kulkarni, *Mater. Chem. Phys.* 71 (2001) 98.
- [20] Z. Hu, G. Oskam, P.C. Searson, *J. Colloid Interface Sci.* 263 (2003) 454.
- [21] E. Joselevich, I. Willner, *J. Phys. Chem.* 98 (1994) 7628.
- [22] C.B. Murray, D.B. Norris, M.G. Bawendi, *J. Am. Chem. Soc.* 115 (1993) 8706.
- [23] F.M. Moghaddam, M.G. Dekamin, *Tetrahedron Lett.* 41 (2000) 3479.
- [24] F.M. Moghaddam, H. Porkaleh, H. Zali-Boinee, *Lett. Org. Chem.* 3 (2006) 123.
- [25] F.M. Moghaddam, H. Zali-Boinee, *Tetrahedron Lett.* 44 (2003) 6253.
- [26] F.M. Moghaddam, M. Ghafarzadeh, *Synth. Commun.* 31 (2001) 317.
- [27] F.M. Moghaddam, H. Isamaili, G. Rezanejad, *Hetroatom Chem.* 17 (2006) 136.
- [28] B. Dubertret, P. Skourides, D.J. Norris, V. Noireaux, A.H. Brivanlou, A. Libchaber, *Science* 298 (2002) 1759.
- [29] JCPDS diffraction database: Zincite [36-1451].
- [30] B.D. Cullity, S.R. Stock, *Elements of X-ray Diffraction*, third ed., Prentice-Hall, Englewood Cliffs, New Jersey, 2001.
- [31] H.M. Chang, H.C. Hsu, S.L. Chen, W.T. Wu, C.C. Kao, L.J. Lin, W.F. Hsieh, *J. Cryst. Growth* 277 (2005) 192.
- [32] Q. Zhong, E. Matijevic, *J. Mater. Chem.* 6 (1996) 443.
- [33] S. Maensiri, P. Laokul, V. Promarak, *J. Cryst. Growth* 289 (2006) 102.
- [34] K. Tanabe, *Solid Acids and Bases*, Academic Press, New York, 1970.
- [35] F. Tamaddom, M.A. Amrollahi, L. Sharafat, *Tetrahedron Lett.* 46 (2005) 7841.
- [36] M. Gupta, S. Paul, R. Gupta, A. Loupy, *Tetrahedron Lett.* 46 (2005) 4957.
- [37] M. Hosseini-Sarvari, H. Sharghi, *J. Org. Chem.* 71 (2006) 6652.